

## ANALYSIS OF THE QUASI-STATIC RIVETING PROCESS FOR 90° COUNTERSUNK RIVET

Jerzy Kaniowski  
Wojciech Wronicz

*Institute of Aviation, Warsaw, Poland*

### 1. INTRODUCTION

Riveting is the most commonly used method of joining sheet metal components of the aircraft structure. The riveted joints are critical areas of the aircraft structure due to severe stress concentrations and effects such as fretting and secondary bending. The most spectacular and well-known evident of this was the accident of Boeing B737 of Aloha Airline in 1988, when during the flight at altitude of 7300 m a large part of fuselage skin was removed due to explosive decompression. The investigation showed that the reason for this accident was widespread fatigue damage of riveted joints. This accident was an impulse for establishing many research programs around the world focused on fatigue of riveted joints. In the Netherlands, the University of Technology in Delft was one of active centres where fatigue of riveted joints was a subject of numerous investigations and PhD dissertations, among other the one presented by R.P.G. Müller [1]. He showed that there is strong correlation between riveting force and fatigue life of riveted joints. In the case of three-rows riveted joints assembled with the squeezing force value (driven head dimension) according to the industrial manual fatigue life varied between 39 630 cycles for minimum and 95 200 for nominal squeezing force values. For high squeezing force fatigue life of joint was 446 413 (fig. 1).

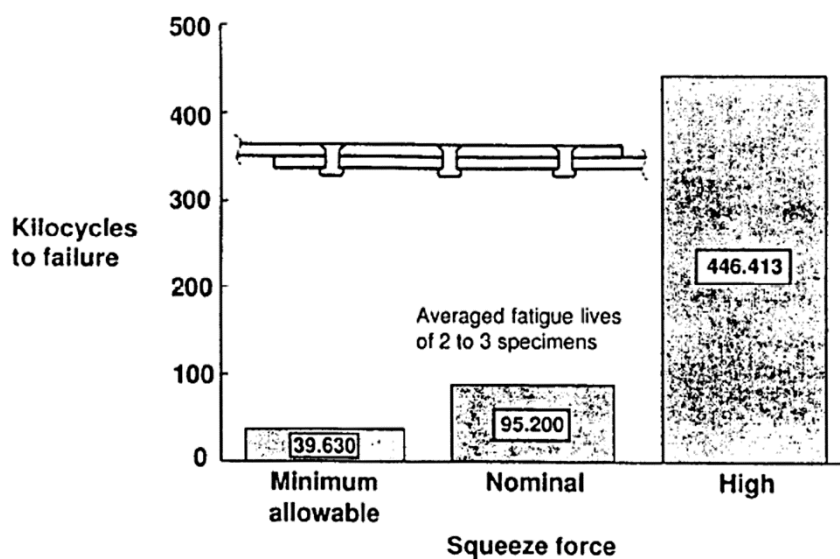


*Fig. 1 Influence of squeezing force value on fatigue life of riveted joints [2]*

Fatigue life of such joints depends also on the rivet type, which has been presented by R.F. Simenz and M.A. Stainberg [3], fig. 2.

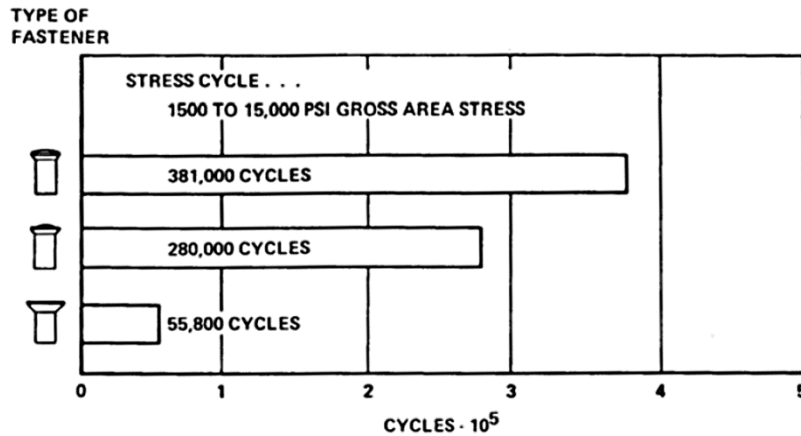


Fig. 2. Influence of rivet type on fatigue life of riveted joints [3]

In Poland, the fatigue program was carried out at the Institute of Aviation during the years 1980-1998 as part of design and development works on the training-combat jet I-22 Iryda [4],[5]. Squeezing force as well as a rivet type influence directly stress and strain fields around the rivets generated during the riveting [1],[6],[7]. Compressive stresses prevent crack nucleation, which extends fatigue life of joints. Determination of stress and strain pattern around the rivet for various rivet types and riveting parameters was an important part of the IMPERJA project, which was devoted to improvement of fatigue life of riveted joints in aircraft structures [6]-[13]. This paper presents experimental and numerical investigations of strains in quasi-static riveting of a countersunk rivet.

## 2. EXPERIMENT

To measure strains in the area of the high stress and strain gradient, which occurs around the rivet due to the riveting process, the specimen presented in fig. 3 was designed and manufactured.

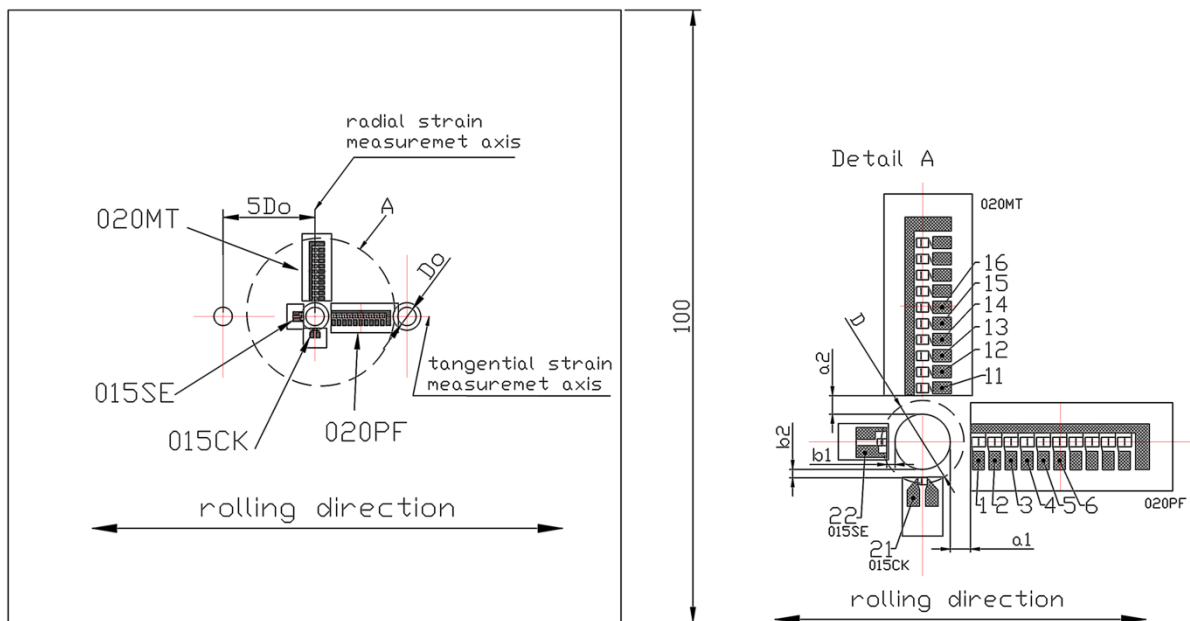
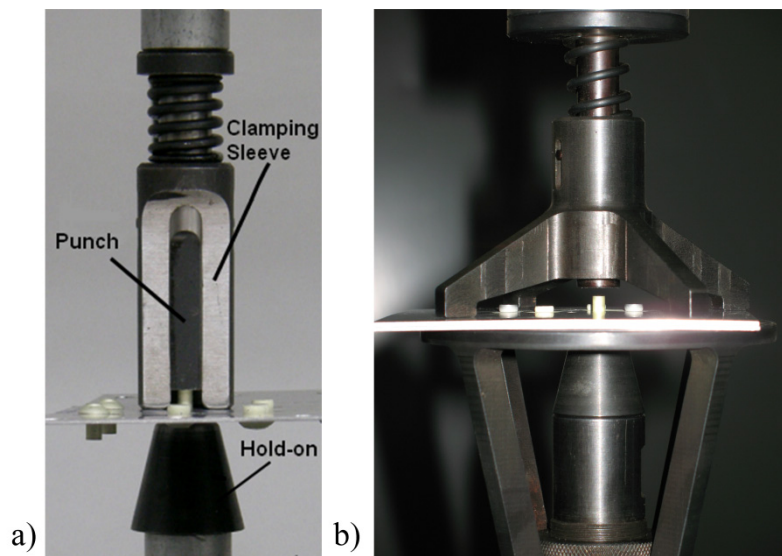


Fig. 3. Specimen geometry

The specimen consists of two bare sheets made from 2024 T3 aluminium alloy with the nominal thickness of 1,27 mm and three 90° countersunk rivets (according to Polish aerospace standard BN-70/1121-04) with the diameter of 3 mm made from Polish aluminium alloy PA25. At the beginning, the outer rivets were installed, afterwards the strain gauges were applied on the sheet surface near the driven head and the central rivet was installed. Strain progress was recorded. Strip and micro gauges were used. The strip miniature gauges containing ten gauges each (six were used), each with gauge length of 0,51 mm, were located outside the driven head. They worked during the whole riveting process. Besides those, two micro strain gauges with gauge length of 0,38 mm were applied very close to the rivet hole, in the area under the driven head. The gauges recorded strain until they were destroyed by the driven head. Riveting of the central rivet was carried out with a special riveting set to avoid damage of the gauges by a clamping sleeve used in the standard riveting set (fig. 4). The squeezing force was equal to 11,42 kN. More information about experiment and calculations (for different types of rivets) can be found at [7].



**Fig. 4. Riveting set a) standard, b) special**

### 3. RESULTS

The recorded strains were shown in figures 5 and 6. The graphs present strains in particular gauges as a function of squeezing force (gauge numbering according to fig. 3). Because of malfunction of one testing card tangential strains of gauge no. 3 were not recorded.

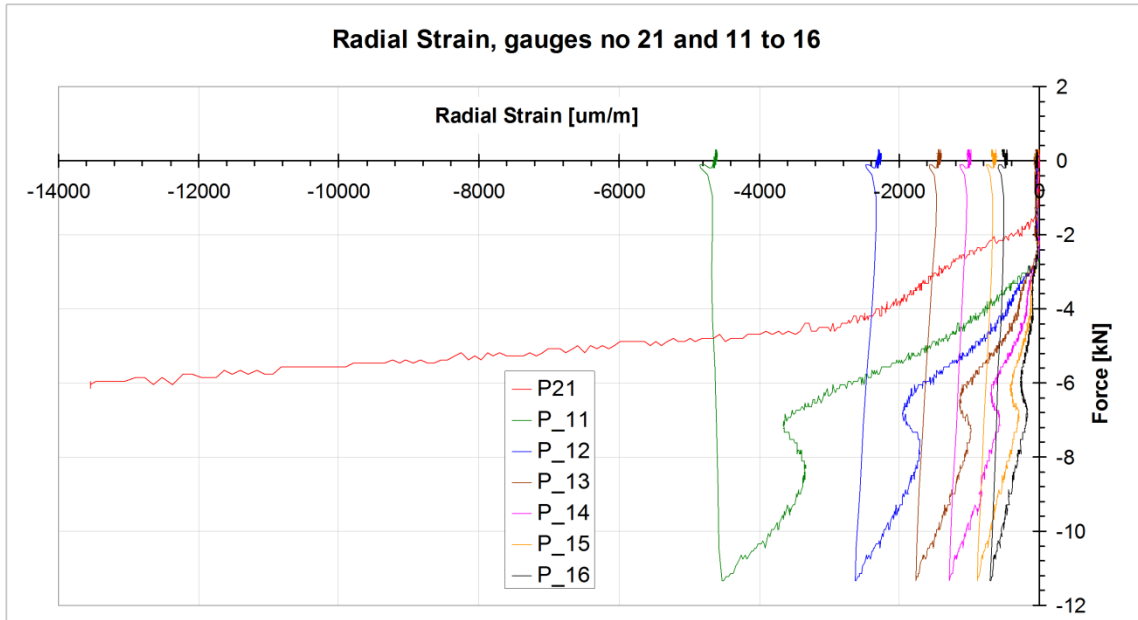


*Fig. 5. Radial strains recorded during the riveting process*

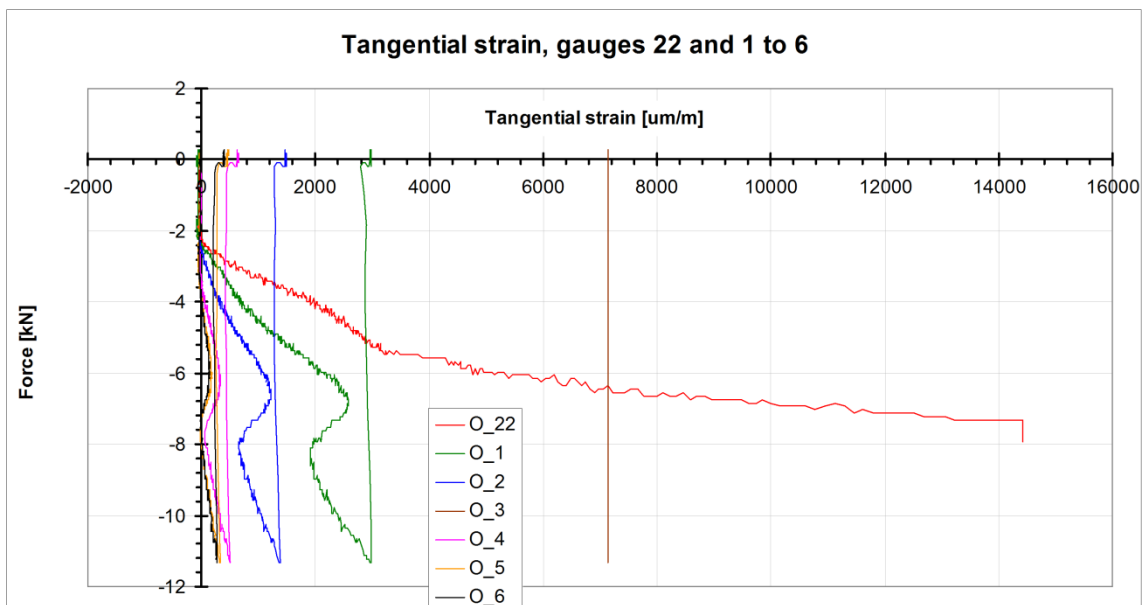
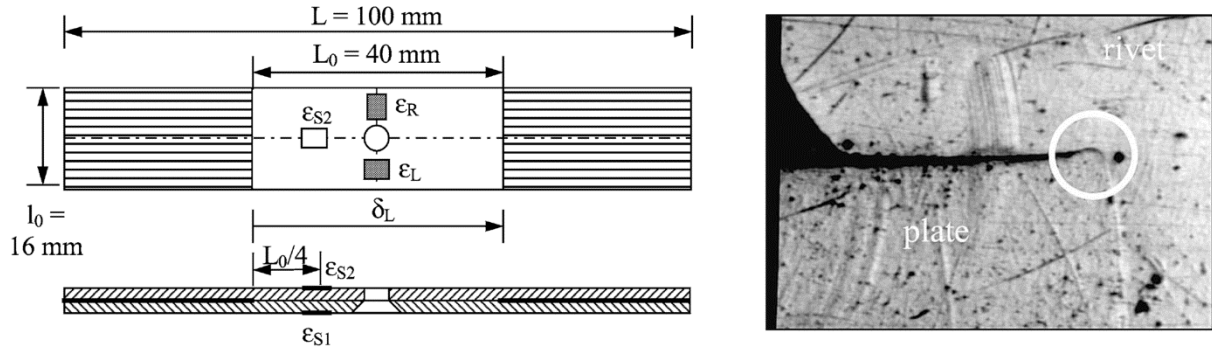


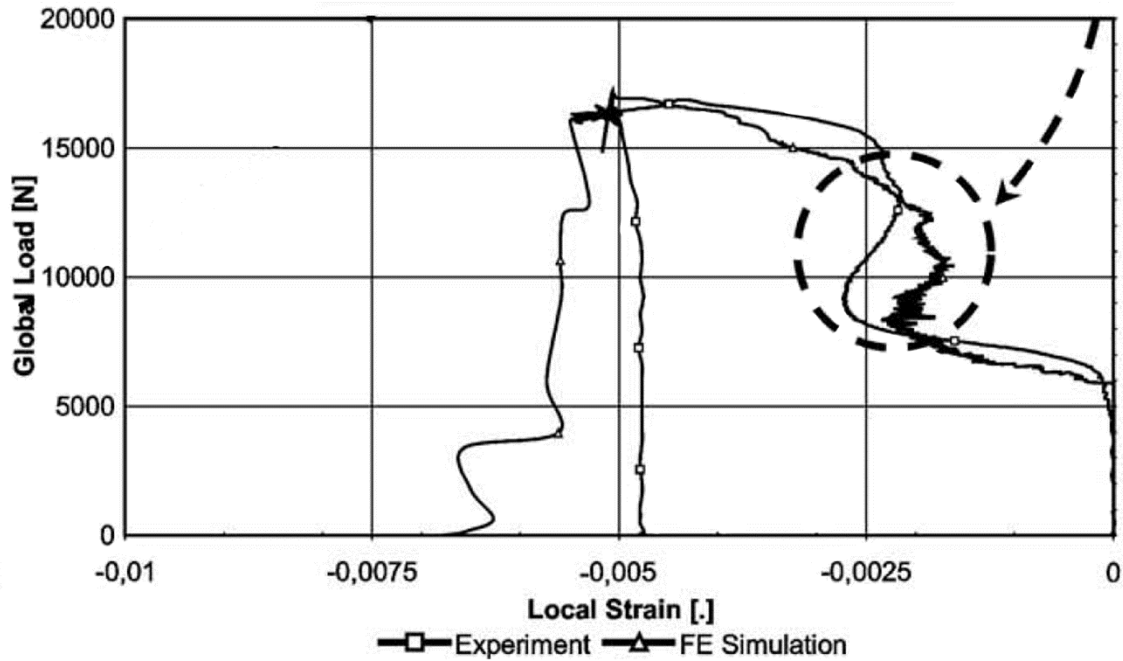
*Fig. 6. Tangential strains recorded during the riveting process*

Strains recorded by micro gauges are very high. The ‘S’ shape strains were recorded by all strip gauges in the case of both the radial and tangential direction. Similar shapes of strain plots were presented by Langrand et al. [14] as well as by Li at al. [15] (fig. 7, 8). Both authors analysed strains during riveting process for countersunk rivets.



a)

b)



c)

Fig. 7. Equivalent strain signal obtained by Langrand et al [14]

Langrand et al. explain reversal strain signal, as a result of the so called ‘lug formation’ on the hole edge, under the driven head (see photo in fig. 7b). Analysis of the microsection of selected specimens riveted at the Institute of Aviation does not confirm the existence of such deformation. The existence of a chamfer on the hole edge prevents its formation. Despite this, the ‘S’- shaped strain signals were recorded.

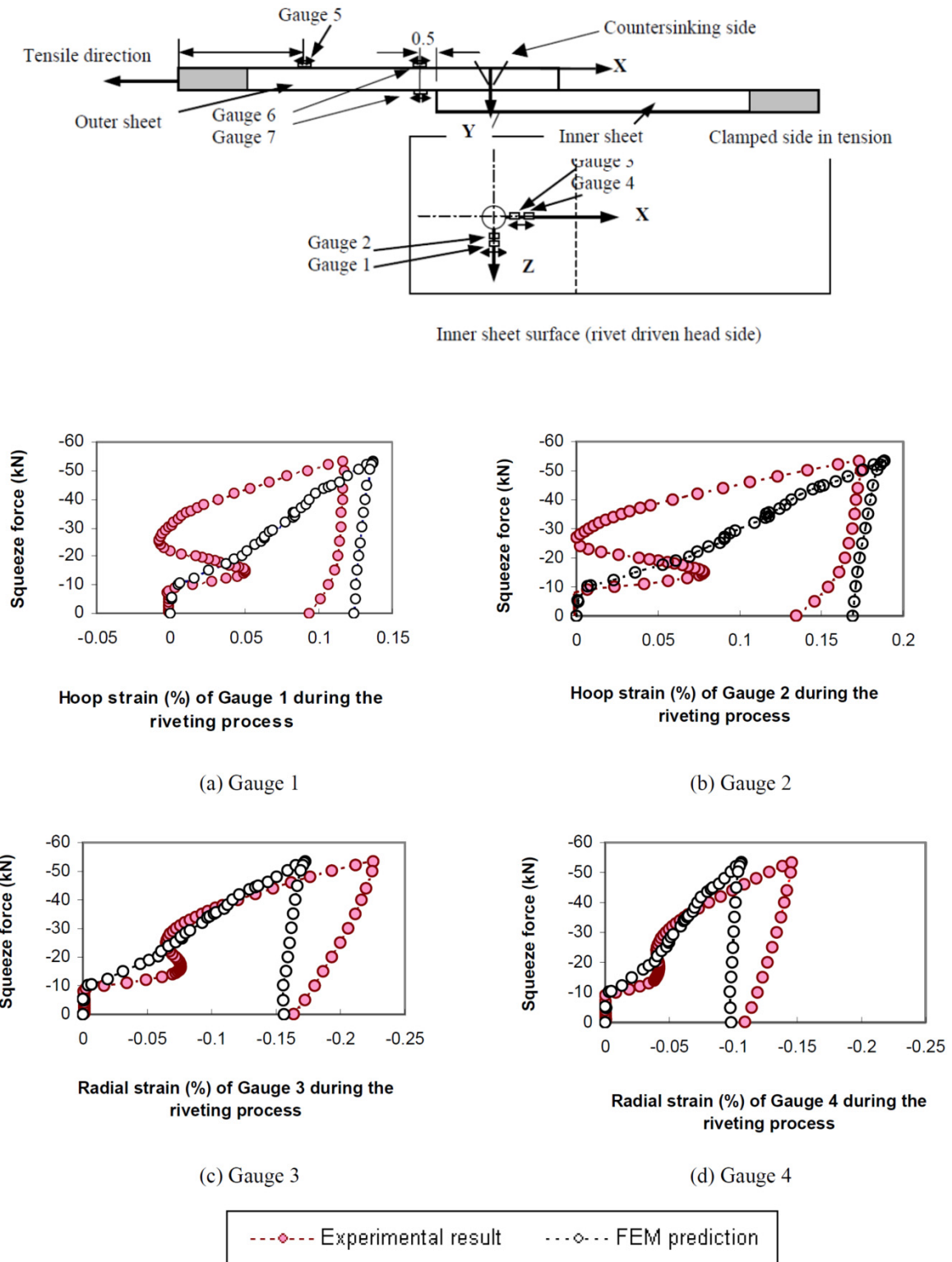


Fig. 8. Strain signals obtained by Li et al [15]

Li et al explain this phenomenon by clearance between the sheet and rivet.

#### 4. NUMERICAL CALCULATIONS

The axisymmetric FEM model was prepared for the analyses of strain and stress field around the rivet. Only the presence of the central rivet was taken into account in the axisymmetric models (the outer rivets were neglected). Moreover, the model represents circular specimen (axisymmetric analysis) with diameter equal to real specimens' side length. Previous analyses with axisymmetric and solid models prove that such simplification is acceptable and does not influence the results near the rivet significantly. The model consists of five contact bodies; three deformable ones (two sheets and a rivet) and two rigid ones that simulate the effect of the hold-on and the press punch. There are 2 132 linear elements and 2433 nodes in the model.

Special boundary conditions resulting from the use of the special riveting set were modelled. The model is presented in fig. 9.

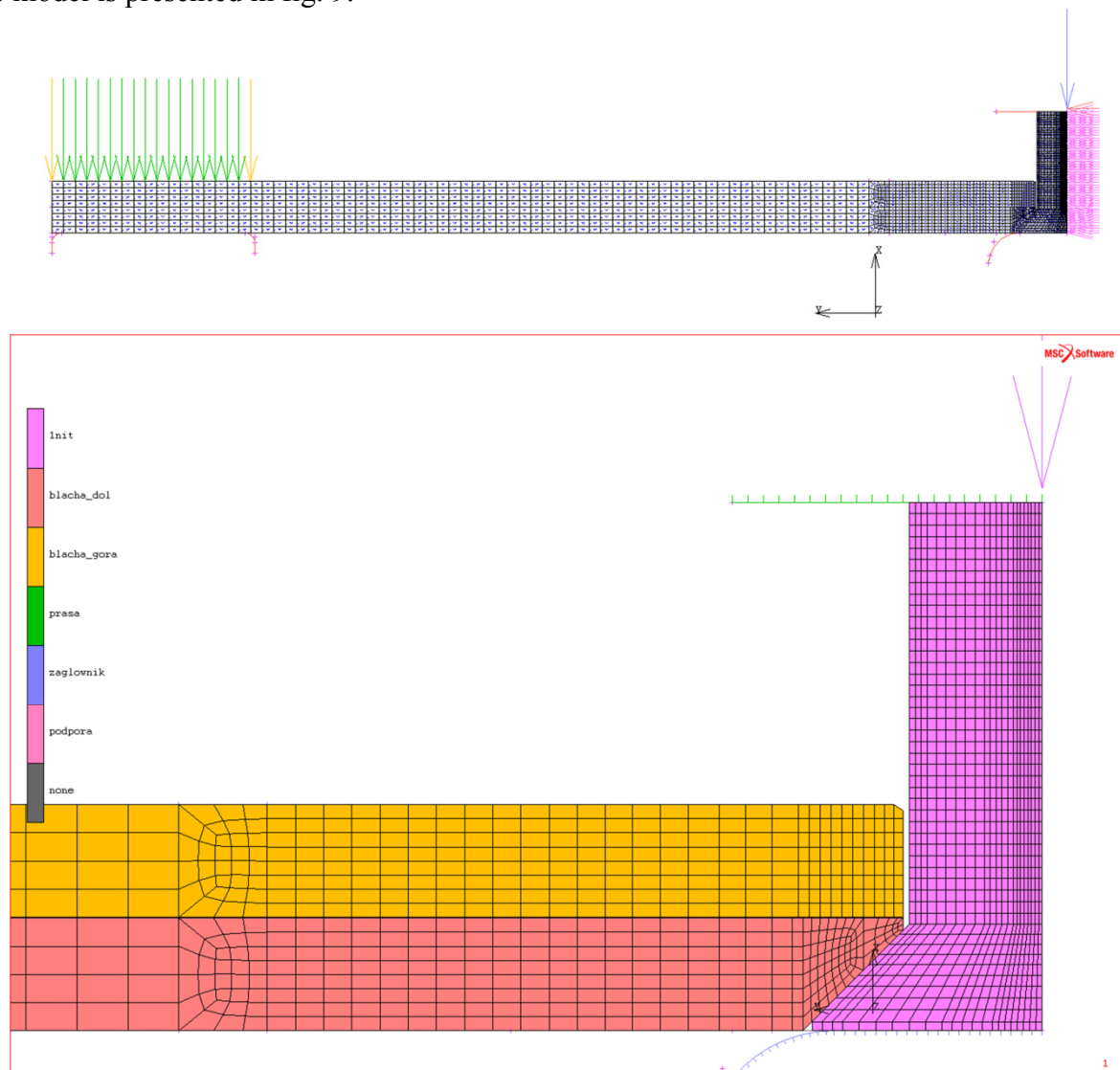


**Fig. 9. Numerical model**

The nonlinear static analysis of the riveting process with force control was performed. The MSC MARC software was used. The models of the materials, developed based on monotonic tests of specimens cut from sheet (2024-T3) and rivets (PA25), were used. The tests were carried out by Prof. Małgorzata Skorupa's team at the AGH University of Science and Technology in Cracow [6]. Help of the company Evektor with the PA25 alloy model development is appreciated. The material models are presented in fig. 10.

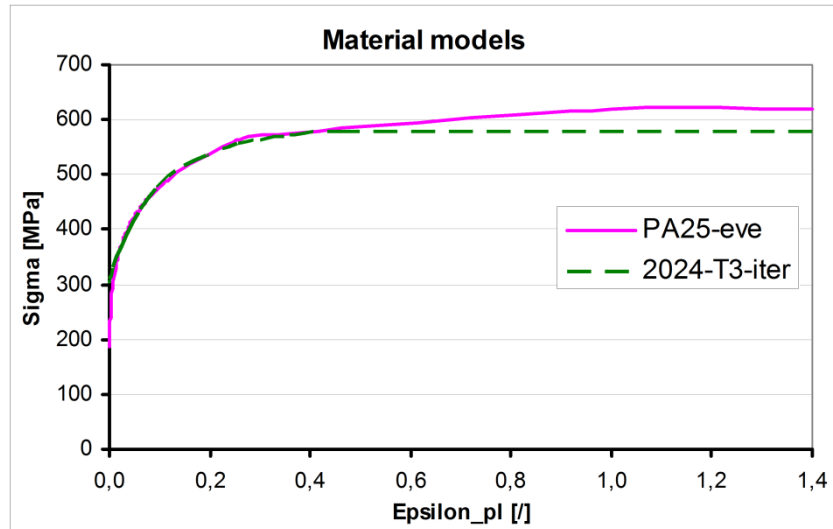


Fig. 10. Material models

A stick-slip Coulomb model of friction was selected. For sheets and sheet-rievet contact pairs, the dynamic friction coefficient value equal to 0.34 was assumed [16]<sup>1</sup>. For contact between the rivet and rigid bodies, the friction coefficient value was 0.15<sup>2</sup>. Static friction coefficients were higher by 24 %<sup>1</sup>.

Fig. 11 presents equivalent stresses (Huber-Mises-Hencky-HMH) and deformation at the end of the process obtained in numerical calculation. Non-uniform stress distribution through the sheets thickness is visible.

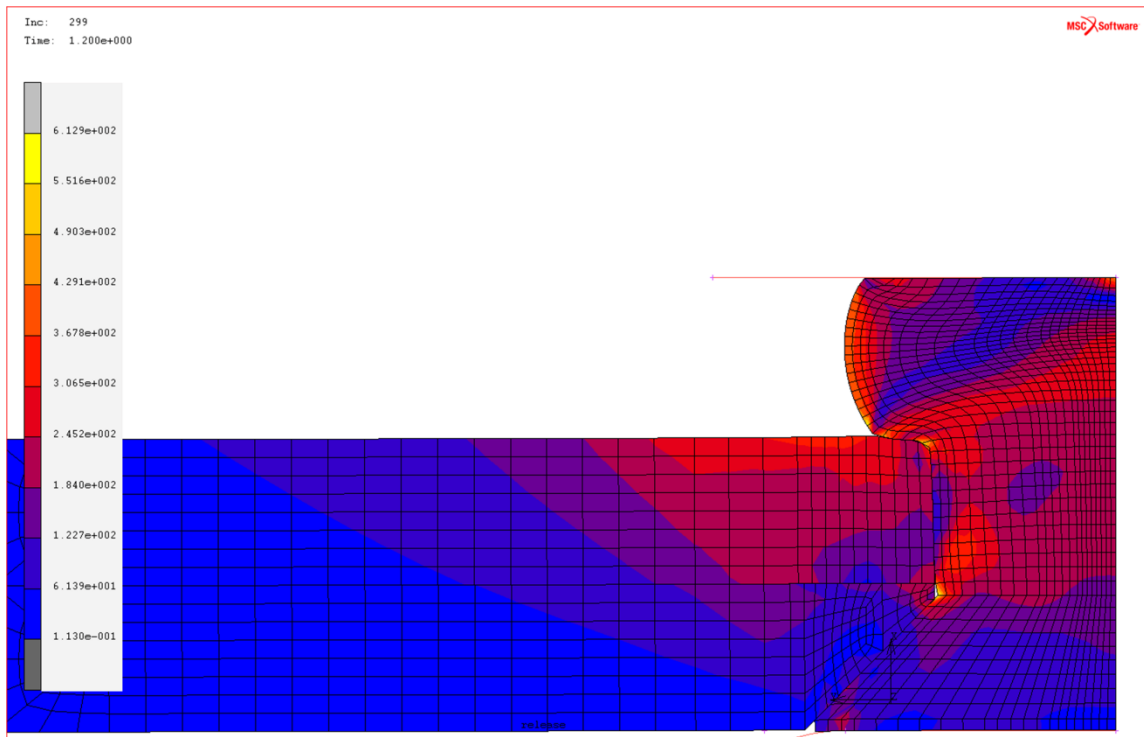


Fig. 11. Equivalent stresses (HMH) and deformation of the model at the end of riveting

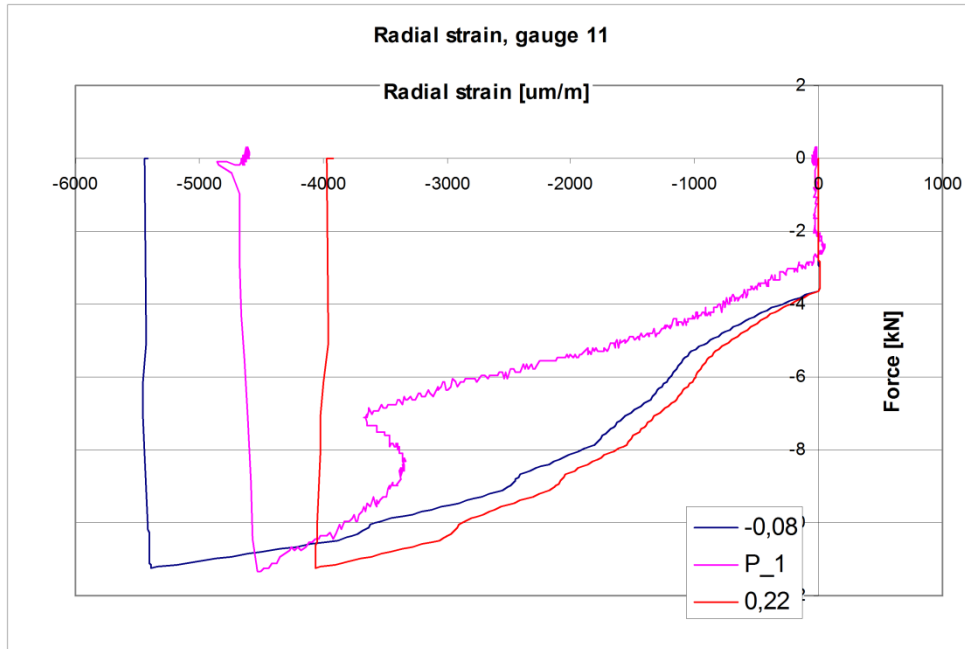
<sup>1</sup> [9] Appendix: Static and Kinetic Friction Coefficients for Selected Material, Table 1, for Al 6061-T6/6061-T6 contact pair.

<sup>2</sup> For the 0.15 value, geometry of the driven head obtained in numerical calculations was the closest to the real dimensions.

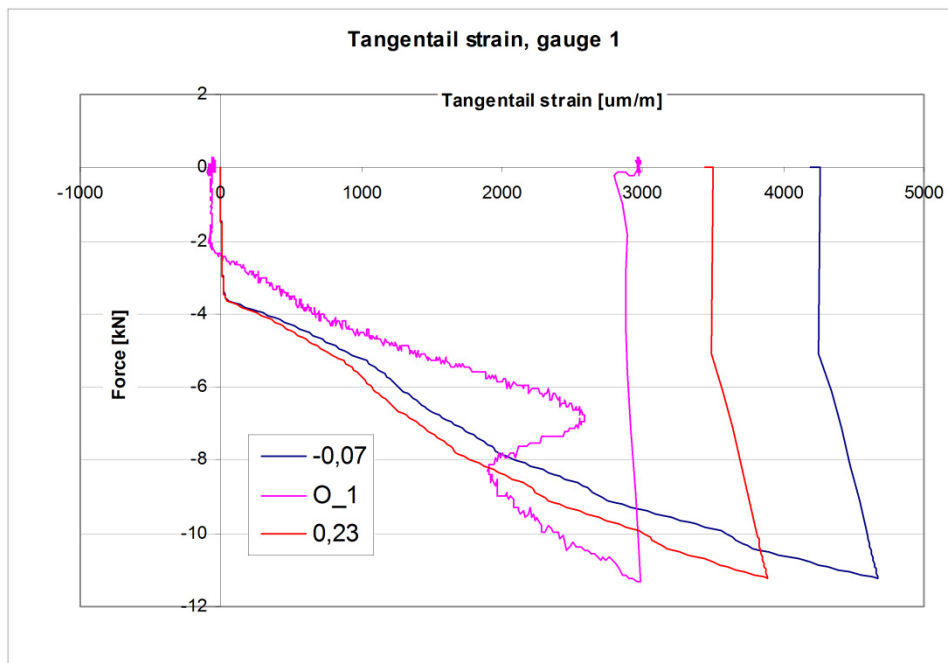


Results (strains) obtained in calculation were compared with the experimental data. Fig. 12. presents strains recorded by strain gauges no. 1 and 11 (see fig. 3) and strains obtained in calculation for nodes located closest to the gauge centre (series name indicate the distance between the radial position of the gauge centre and the node).

The graphs of strain as a function of the radial position is presented in fig. 13.

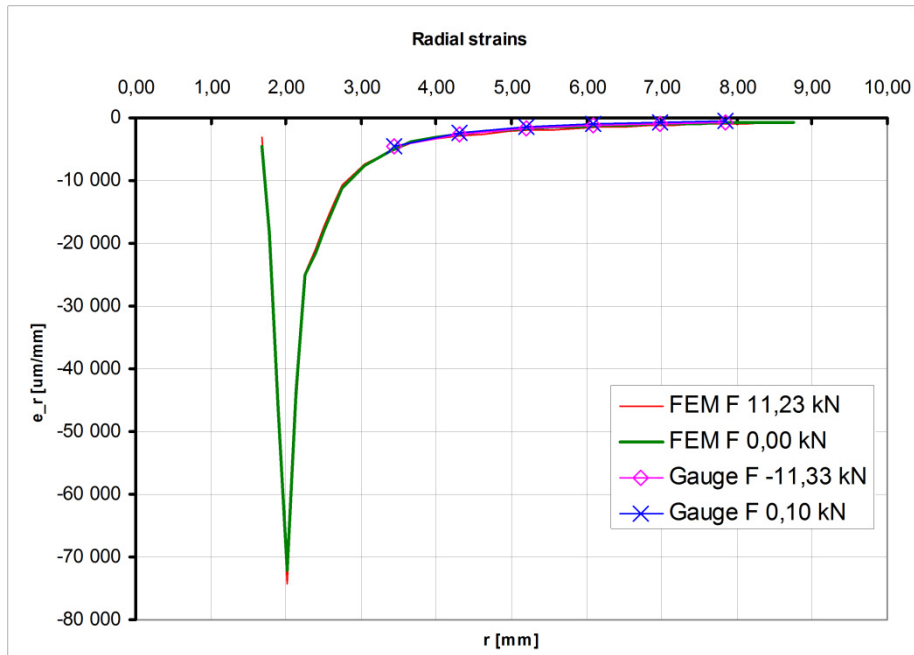


a)

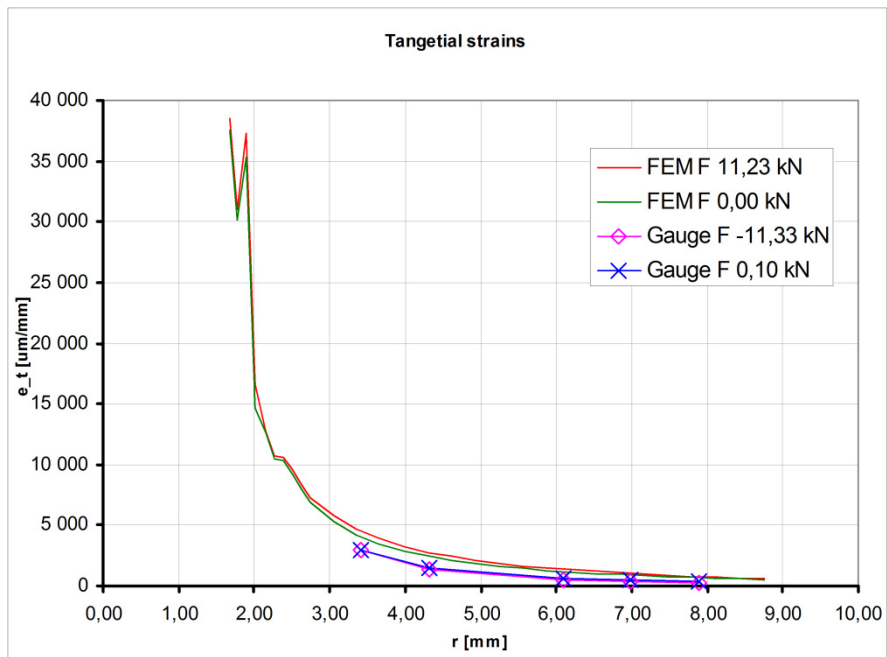


b)

Fig. 12. Strain progress during riveting, a) radial, b) tangential



a)



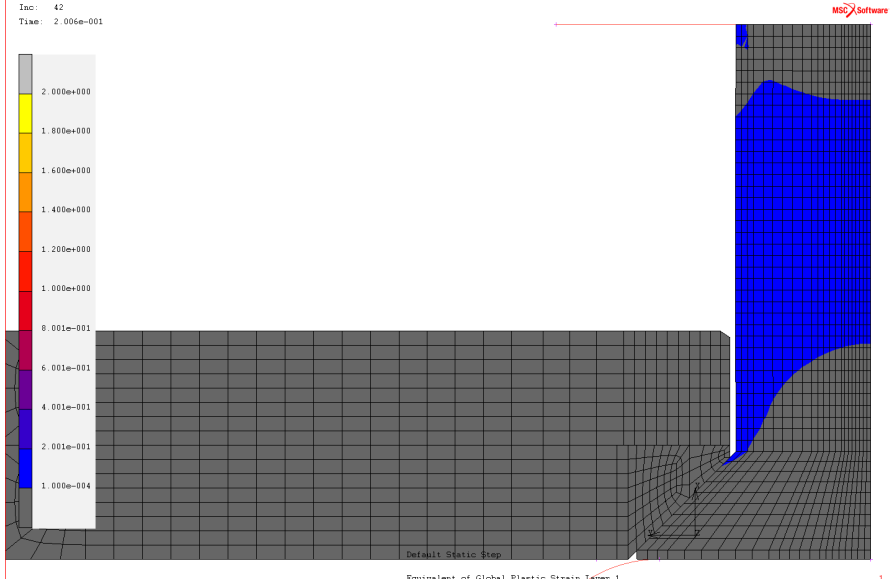
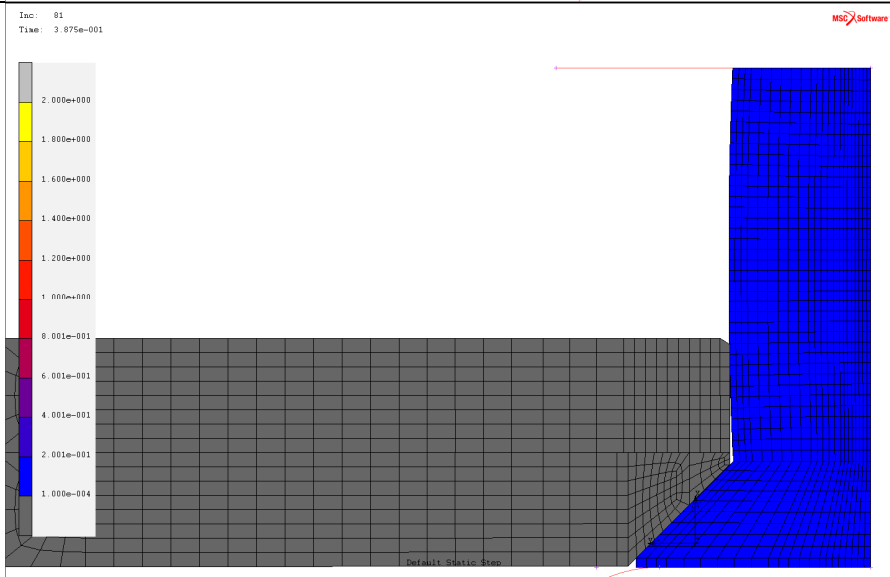
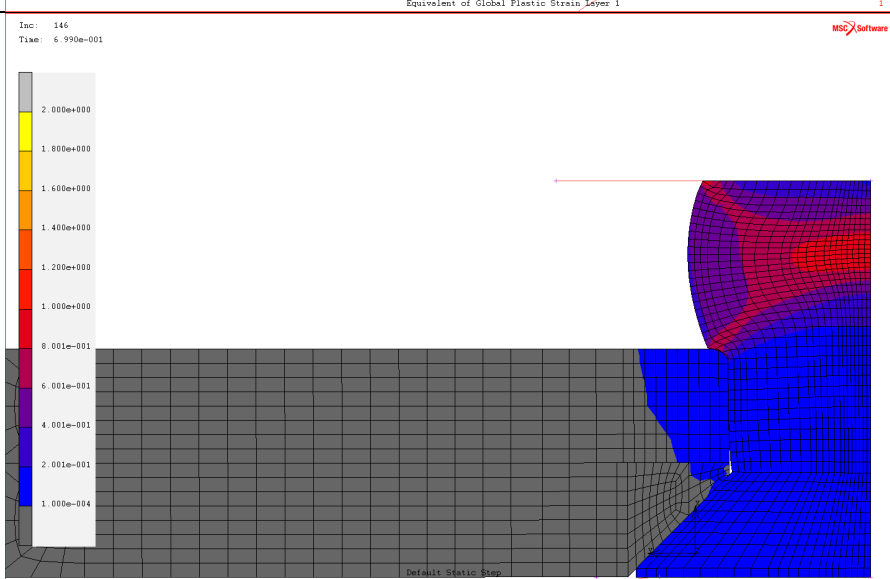
b)

**Fig. 13. Strain as a function of the radial position for maximum force (11,23 kN) and after riveting a) radial strain, b) tangential strain**

In the case of radial strains, good correlation with the experiment at the end of the process is visible. In the case of tangential strains, numerical results are overestimated. During the riveting process the numerical model did not agree with the experiment and the reversal strain signal was not obtained in calculations.

Five stages of the riveting process were proposed. Results of the riveting simulation for the moments dividing the process into stages are presented in table 1. Pictures show deformation of the model and equivalent of the plastic strain. Gray colour indicates the elastic range of the material behaviour.

Table 1. Characteristic moments during the riveting process

No.	Description	Results
1.	1,3 kN Most of the rivet shank deformed plastically.	
2.	3,63 kN Rivet shank touch the rivet hole edge	
3.	7,49 kN Both sheets deformed plastically, Some part of the squeezing force is transferred through the sheets which are pressed together by the driven head and manufactured head	

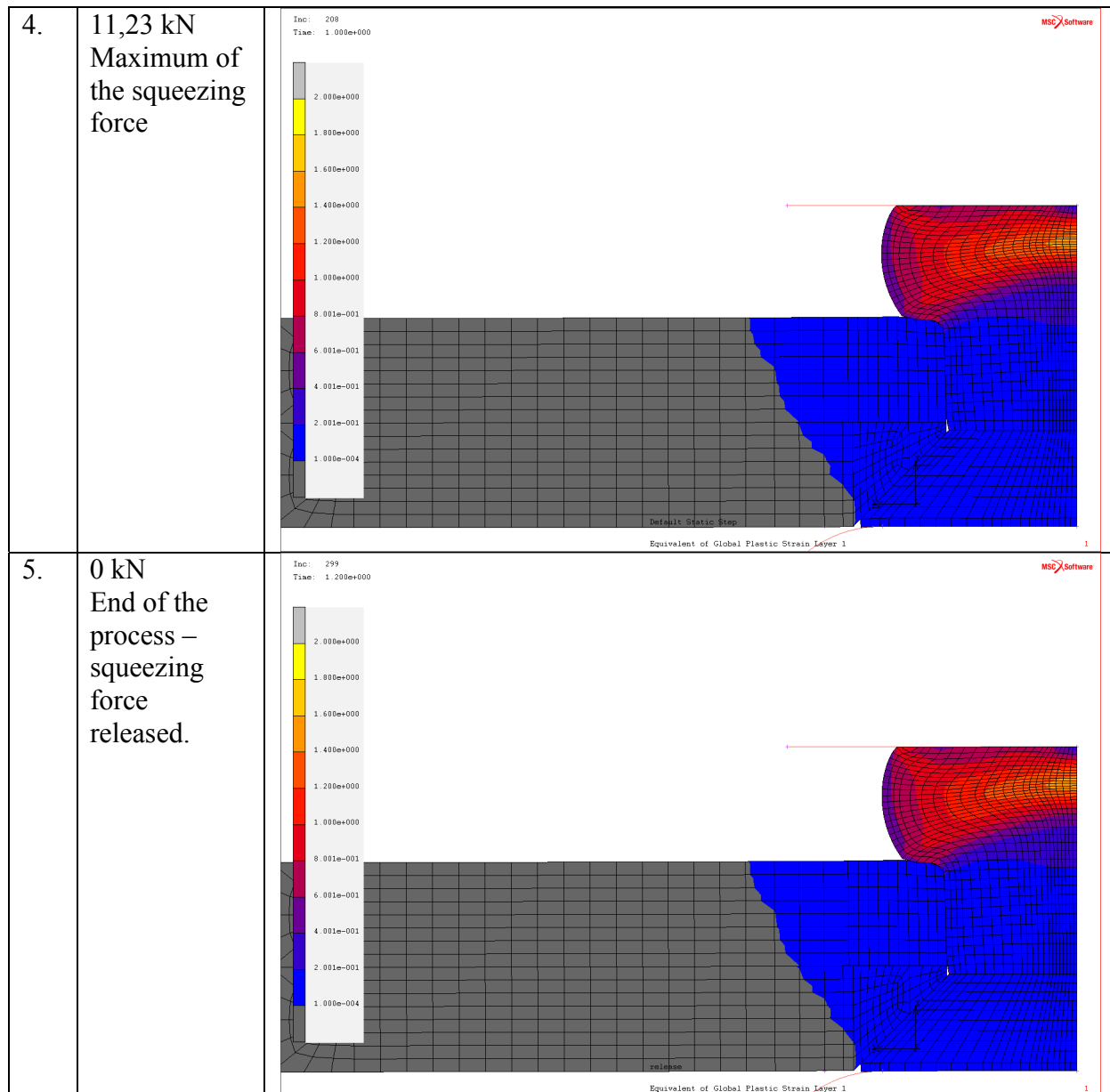


Figure 14 presents the displacement-force curve of the stamp during the riveting process obtained in the experiment and the numerical simulation. Force values for characteristic moments presented in table 1 were indicated. It is visible that the numerical model is too rigid and for the same force stamp displacement obtained in simulation is smaller than the real one. This is connected with the material model of the rivet used in the calculations. This model was developed based on the monotonic tests which were carried out with the specimens cut from the 5 mm diameter rivets while the presented rivets have 3 mm diameter. To verify this hypothesis an additional calculation of the 5 mm rivet (different type) was conducted and results were compared with the measurements. Good correlation was obtained. This shows that general material characteristics available in the literature are not sufficiently accurate for a detailed analysis of the riveting process.

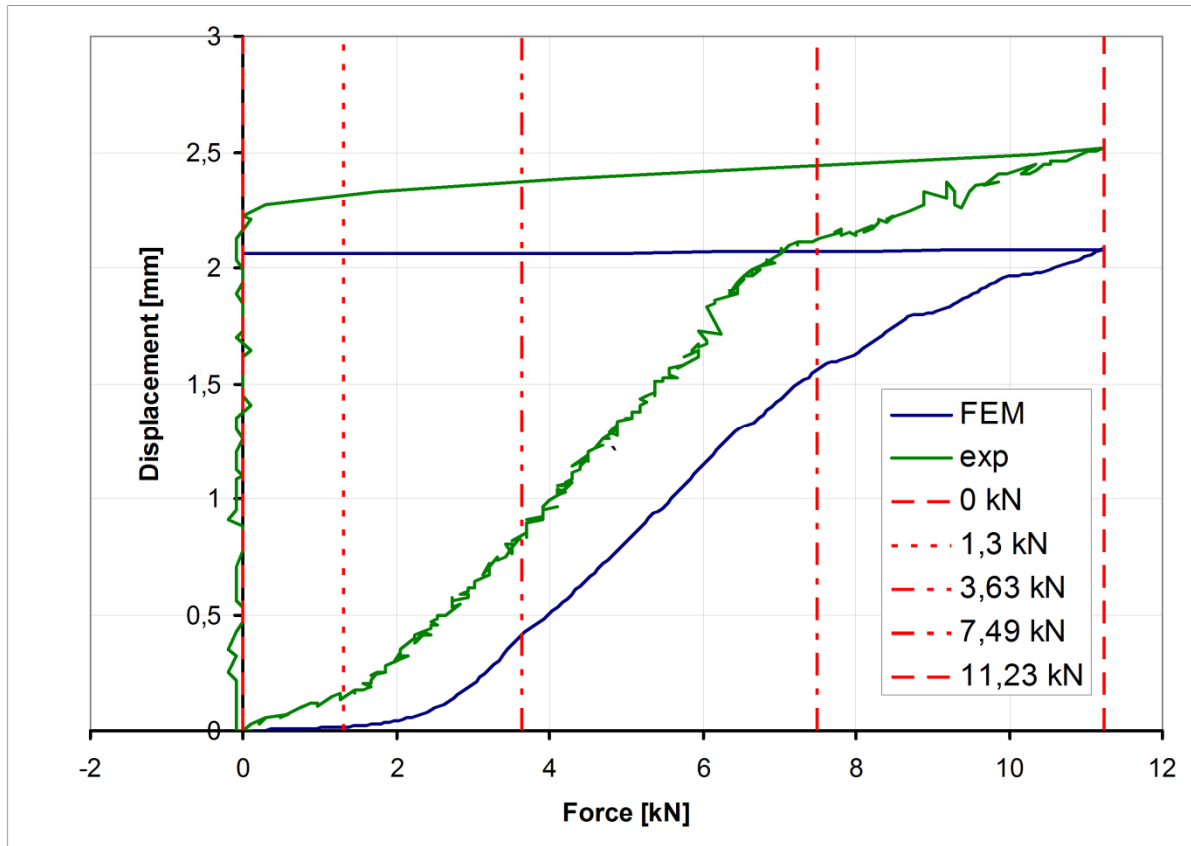


Fig. 14. Displacement-force curve of the stamp during the riveting process

Figure 15 presents graphs of radial and tangential strains as well as punch displacements as a:

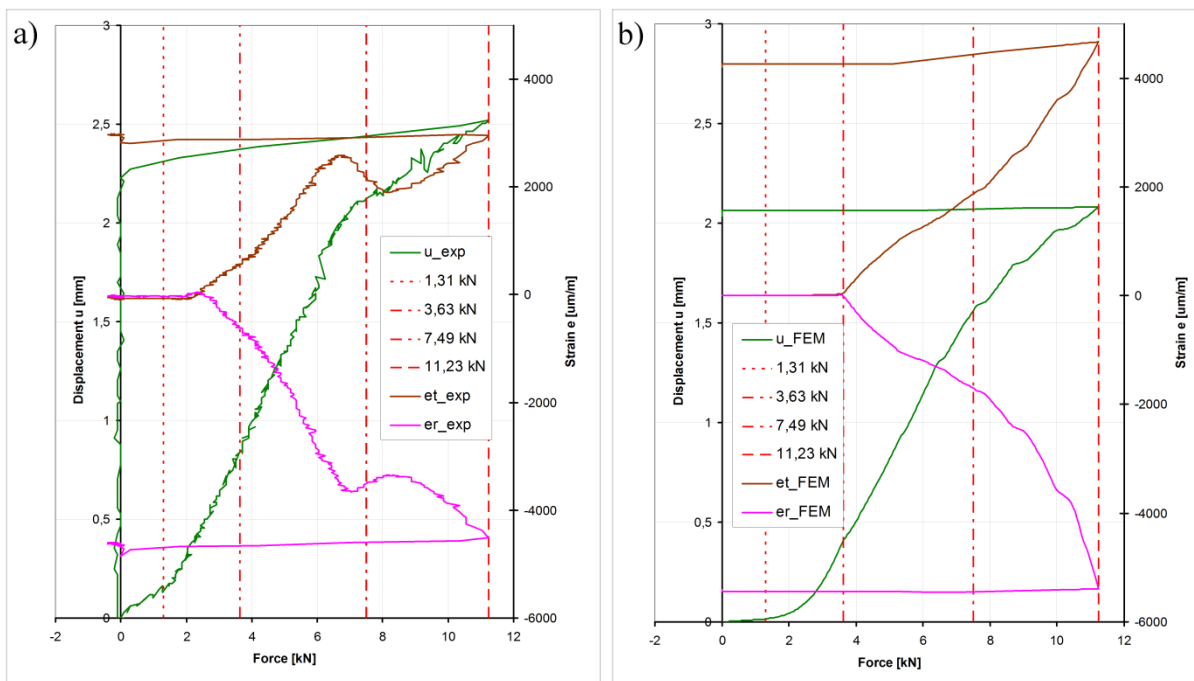


Fig. 15. Strains ( $e_r$ -radial,  $e_t$ -tangential) and punch displacements as a function of riveting force, a) experiment, b) calculations

In the case of numerical calculation, the force level of the second characteristic point (3,63 kN) corresponds with a rapid increase in strain signals. In the experiment, a different force level recorded when strain increase occurs is probably connected with insufficient accuracy of the material model.

The reversal of strain signal recorded during the experiment took place near the load level of the third characteristic point (7,49 kN). It is probable that for an appropriate material model the load level of the third characteristic point will correspond much better with this phenomenon. It suggests that reversal strain signal occurred at the beginning of the driven head forming and when stresses in both sheets exceed yield point.

It is known that an increase in riveting force results in higher fatigue life of riveted joints [1]. The analysis of the Müller and Hart-Smith results [2], has indicated that when a 1,42-time increase in the squeezing force resulted in a twofold increase in the fatigue life, then a three-time increase in the squeezing force resulted in an eleven-time increase, and in case of riveting with the NACA technology, even an eighty-time increase in the fatigue life (see table 2). The magnitude of the life increase suggests that the change of the joint formation mechanism has taken place.

**Table 2 Fatigue life of specimens depending of squeezing force and rivet type [2]**

Rivet type	Squeezing Force [kN]		D/D <sub>0</sub>	No of cycles to failure
	Minimal	12		
Countersunk – 100° angle	Nominal	17	1,4	41 552
				37 226
				40 112
	High	36	1,7	97 535
				99 624
				88 442
Brazier	36	1,7	451 270	
			441 556	
Brazier, riveted upside down <sup>1)</sup>	36	1,7	483 714	
			491 998	
				>3 000 00
				0

<sup>1)</sup> NACA technology.

The working hypothesis has been assumed that during the riveting process adhesive joint (called cold welding) were formed and destroyed during the process, what was the reason of the observed reversal strain signal. According to the literature [17], [18] a contact stress level of 380 MPa is necessary for occurrence of this type of joint. The fig. 16 presents contact normal stresses on the rivet-sheets interface for characteristic load levels. The path along which stresses are presented was mark as a black line with an arrow on the picture of the FEM model (fig. 16a). Stresses exceed 380 MPa at some area of cylindrical as well as countersunk part of the hole for the maximum force. This fact intimates that formation of cold welding joints is possible.

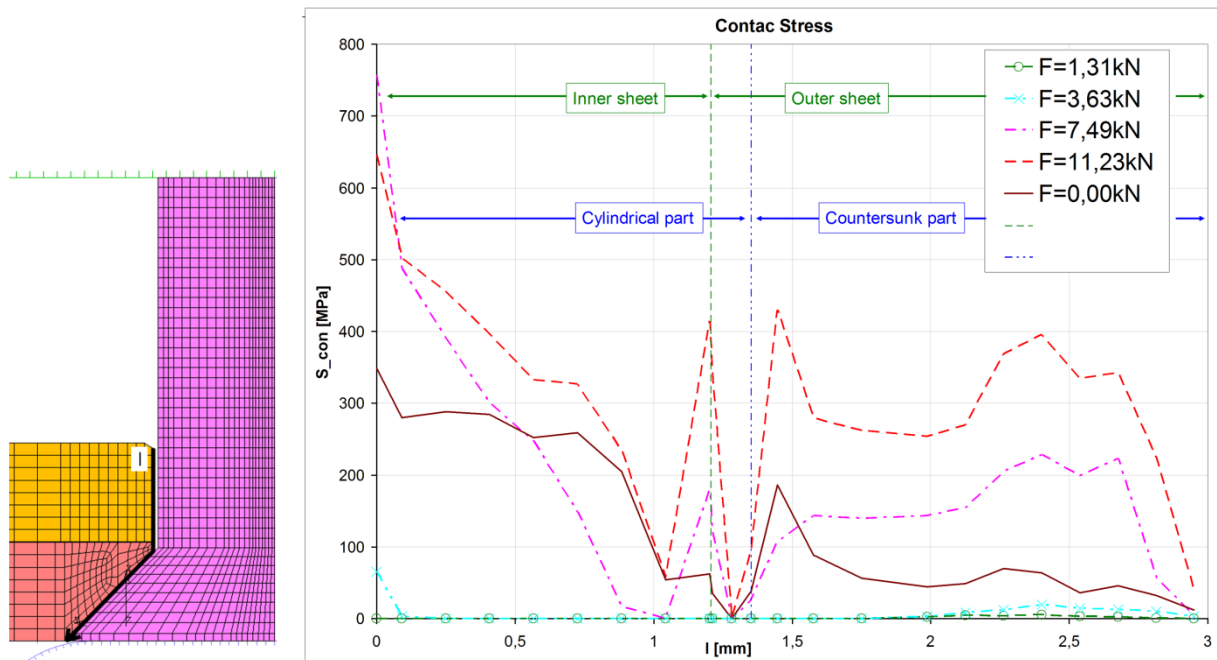


**Fig. 16.** Contact normal stresses on the rivet-sheets interface for characteristic load levels

## 5. CONCLUSIONS

The paper presents experimental and numerical investigations into the stress and strain state during the riveting process. This state has crucial influence on the fatigue performance of riveted joints. The analyses and FEM calculations were performed for countersunk solid rivets with strain gauges. Five characteristic moments of the riveting process were distinguished. The reversal strain signal during the riveting process was recorded in the measurements. This phenomenon was not observed in numerical calculations. The working hypothesis was assumed that between the rivet and sheets cold welding joints were formed and destroyed during the riveting process, which resulted in reversal strain signal. This phenomenon was not represented in the calculations. The numerical analysis of contact normal stresses between the rivet and sheets showed that in some regions stresses exceeded the level necessary for joint formation of this type. Further research is necessary to confirm the existence of cold welding joints as a result of the riveting process.

*Experimental research was carried out as part of the Eureka project E!3496 IMPERJA.*

## REFERENCES

- [1] Muller R. (1995). *An Experimental and Analytical Investigation on the Fatigue Behaviour of Fuselage Riveted Lap Joint*. Ph.D. thesis, TU Delft, Netherlands.
- [2] Müller R. P.G., Hart-Smith L.J.: *Making fuselage riveting lap splices with 200-year crack-free fatigue life*. ICAF 97' Fatigue in new and ageing aircraft. Proceedings of the 19<sup>th</sup> Symposium of the International Committee of Aeronautical Fatigue 1997, Edinburgh, EMAS Publishing, pp. 499-522.
- [3] Simenz R. F., Steinberg M. *Alloy Needs and Design: the Airframe, In Fundamental Aspects of Structural Alloy Design*. Proceeding of the 10<sup>th</sup> Battelle Colloquium in the Materials Science, Jaffee R. I., Wilcox B. (Ed), A, PLENUM PRESS, New York and London 1977.

- [4] Dębski M. (1995). *Metoda oceny trwałości zmęczeniowej struktur nośnych samolotów (Methods of Fatigue Life estimation of Airframes)*. PhD thesis, PW Warszawa, Poland.
- [5] Kaniowski J. (1998). *Badania wpływu geometrycznych cech konstrukcyjnych na trwałość zmęczeniową na przykładzie skrzydła samolotu PZL I-22 Iryda (The Study of the Influence of Geometric Features on the Fatigue Durability on the Example of the PZL I-22 IRYDA Plane Wing)*. PhD thesis, ATR Bydgoszcz, Poland.
- [6] Skorupa M, Skorupa A, Michniewicz T, Korbel A. Effect of production variables on the fatigue behaviour of riveted lap joint. *International Journal of Fatigue*, 32 (2010), pp. 996-1003
- [7] Wronicz W., Kaniowski J., Experimental and Numerical Study of Strain Progress During and After Riveting Process for Brazier Rivet and Rivet with Compensator – squeezing force and rivet type effect. In A. Niepokólczycki (Ed.), *Fatigue of Aircraft Structures*, ISSUE 2011 (pp. 165-189). Warsaw: Institute of Aviation Scientific Publication.
- [8] Gadalińska E., Wronicz w., Kaniowski J., Korzeniewski B.: Calculation and Experimental Verification of Residual Stresses in Riveted Joints Used in an Airframe. In A. Niepokólczycki (Ed.), *Fatigue of Aircraft Structures*, ISSUE 2010 (pp. 23-36). Warsaw: Institute of Aviation Scientific Publication.
- [9] Skorupa M., Skorupa A., Machniewicz T., Korbel A.: *An Experimental Investigation on the Fatigue Performance of Riveted Lap Joints*. ICAF2009, Bridging the Gap between Theory and Operational Practice. Proceedings of the 25th Symposium of the Int. Committee on Aeronautical Fatigue, Rotterdam, The Netherlands, 27-29 May 2009. Editor M.J. Bos, Springer, 2009, pp. 449-474.
- [10] Szala J.(Ed.), Boroński D., Lipski A, Mroziński S. *Metody doświadczalne w badaniach materiałów stosowanych na poszycia samolotów i połączeń nitowych. Wybrane zagadnienia (Experimental Methods in Test of Materials for Aircraft Skin and Riveted Joint. Selected Problems)*. Wydawnictwa Naukowe Instytutu Technologii i Eksploatacji – PIB w Radomiu, Radom, 2010, ISBN 978-83-7204-950-6.
- [11] Szymczyk E., Jachimowicz J., Sławiński G., Derewońko A., *Influence of technological imperfections on residual stress fields in riveted joint*. Dissipation and Damage across Multiple Scales in Physical and Mechanical Systems, Oxford, United Kingdom, 2009, 1, 118, pp. 1-4.
- [12] Papuga J. (2010). Fatigue Prediction Based on Finite Element Analysis of Riveted Joints. Czech Aerospace Proceedings, *Journal For Czech Aerospace Research*, No. 3, Vol. 2010, pp. 27-31.
- [13] Fárek J. (2010). *FE-Modelling Methodology of Riveted Joints*. Czech Aerospace Proceedings. Journal For Czech Aerospace Research, No 2/2010, pp. 12-16.
- [14] Langrand B., Patronelli L., Deletombe E., Markiewicz E., Drazétic P., An alternative numerical approach for full scale characterisation for riveted joint design. *Aerospace Science and Technology*, Vol 6, 2002, pp. 343-354.
- [15] Li G., Shi G., Berlinger N.C., *Studies of Residual Stress in Single-Row Countersunk Riveted Lap Joints*. 46<sup>th</sup> AIAA/ASME/ASCE/AHS/ASC Structures, Structural Dynamics & Materials Conference 18 - 21 Apr 2005, Hyatt Regency Austin, Austin, Texas
- [16] ASM Handbook, Volume 18, *Friction, Lubrication, and Wear Technology*, 1995.
- [17] Stojman I.M.: *Cholodnaja svarka metallov*. Mašinostrojenje, 1985, pp.38 and 51.
- [18] Sachackij G.P.: *Technologia svarki metellov w cholodnom sostojanii*, Naukowa Dumka 1979, p.111.